Plasma Proteins Adsorption Mechanism on Polyethylene-Graft-Poly(Ethylene Glycol) Surface by Quartz Crystal Microbalance with Dissipation.

ARTICLE *in* LANGMUIR · MAY 2013

Impact Factor: 4.46 · DOI: 10.1021/la4017239 · Source: PubMed

5 AUTHORS, INCLUDING:

Jing Jin
Linköping University
33 PUBLICATIONS **292** CITATIONS
SEE PROFILE

Paola Stagnaro
Italian National Research Council
90 PUBLICATIONS **793** CITATIONS
SEE PROFILE

Langmuir

Article

pubs.acs.org/Langmuir

Plasma Proteins Adsorption Mechanism on Polyethylene-Grafted Poly(ethylene glycol) Surface by Quartz Crystal Microbalance with Dissipation

Jing Jin,[†] Wei Jiang,*[,†] Jinghua Yin,*[,†] Xiangling Ji,[†] and Paola Stagnaro[‡]

[†]State Key Laboratory of Polymer Physics and Chemistry, Changchun Institute of Applied Chemistry, Chinese Academy of Sciences, Changchun 130022, PR China

[‡]Istituto per Io Studio delle Macromolecole, Consiglio Nazionale delle Ricerche, Via de Marini 6, 16149 Genova, Italy

Supporting Information

ABSTRACT: Protein adsorption has a vital role in biomaterial surface science because it is directly related to the hemocompatibility of blood-contacting materials. In this study, monomethoxy poly(ethylene glycol) (mPEG) with two different molecular weights was grafted on polyethylene as a model to elucidate the adsorption mechanisms of plasma protein through quartz crystal microbalance with dissipation (QCM-D). Combined with data from platelet adhesion, whole blood clotting time, and hemolysis rate, the blood compatibility of PE-g-mPEG film was found to have significantly improved. Two adsorption schemes were developed for real-time monitoring of protein adsorption. Results showed that the preadsorbed bovine serum albumin (BSA) on the surfaces of PE-g-mPEG films could effectively inhibit subsequent adsorption of fibrinogen (Fib). Nonspecific protein adsorption of BSA was determined by surface coverage, not by the chain length of PEG. Dense PEG brush could release more trapped water molecules to resist BSA adsorption. Moreover, the preadsorbed Fib could be gradually displaced by high-concentration BSA. However, the adsorption and displacement of Fib was determined by surface hydrophilicity.

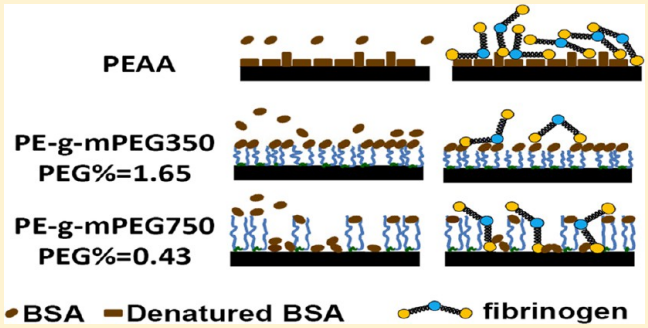

1. INTRODUCTION

Protein adsorption has a vital role in the interface between blood and artificial surfaces because it is directly related to the blood compatibility of blood-contacting medical devices.[1] Adsorption of plasma proteins, such as albumin and fibrinogen (Fib), on the surface of blood-contacting material occurs first, followed by platelet and leukocyte adhesion, coagulation cascade, red blood cell hemolysis, and thrombus formation. In this process, thrombus formation and hemolysis are the two major complications affecting the use of blood-contacting medical devices.[2] Bovine serum albumin (BSA), generally considered to be nonadhesive to platelets,[3] is a globular albumin with the shape of a slight ellipsoid. In contrast, fibrinogen (Fib) is an adhesive protein with a rod-like structure that has a vital role in coagulation, platelet activation, and aggregation. Studies show that albumin has a thromboresistant ability, whereas Fib promotes platelet adhesion.[4] However, little information is available regarding the dynamic interaction mechanism in the molecular level in terms of protein adsorption at the interface.

Protein adsorption is a complex process involving van der Waals forces, electrostatic and hydrophobic interactions, and hydrogen bonding. The interactions between protein and poly(ethylene glycol) (PEG)-modified surfaces have been studied extensively.[5−7] PEG is widely used in the production of biomaterials because of its high efficiency in resisting protein adsorption, weak immunogenicity, and good compatibility with living cells.[8] However, resistance to the protein adsorption dynamic mechanism of PEG is not well understood because of the effect of several parameters, such as grafting density, chain length, protein size,[9] chain−protein interactions and protein−surface interactions.[10] The protein adsorption mechanism of PEG has been interpreted in terms of steric stabilization, chain mobility, and hydration.[11−13] Furthermore, protein adsorption from blood to PEG-modified surface is not a static, but a dynamic, process.[14] In this process, protein may bind, rearrange, and detach.[15] In addition, proteins exhibit various types of conformation and orientation, as well as different adsorption kinetics, because of diverse PEG-modified surface properties.[16] The conformation of proteins adsorbed on a hydrophobic surface may change from globular to an extended chain.[17] Significant conformational changes in proteins result in denaturation and tertiary structural dissociation. These processes are the most important because initial protein adsorption and subsequent changes mediate and control

Received: November 6, 2012
Published: May 9, 2013

dx.doi.org/10.1021/la4017239 | Langmuir 2013, 29, 6624−6633

further interactions between proteins and PEG molecular chains.[18] Thus, the native conformation and orientation of interacting proteins caused by PEG-modified surfaces should be maintained to design and fabricate blood-compatible materials under solution conditions which are close to the physiological environment.

Quartz crystal microbalance with dissipation (QCM-D) is a powerful surface technique in studying the interactions between proteins and surfaces because measurements are made in real time.[19,20] Aside from providing information on the film mass, this technique can also be used in determining how the PEG chain interacts in the solution, as well as in monitoring the changes in protein adsorption kinetics and physical properties of interfacial PEG chains, such as swelling behavior. The frequency (Δf) and dissipation (ΔD) data analyses provide information on the rate and amounts of adsorbed protein, effective thickness, conformational changes, and hydration state of thin films.[21,22] In addition, a combination of QCM-D and other techniques, such as dual polarization interferometry (DPI),[1] ellipsometry,[23] and neutron reflectivity (NR),[24] have been used to investigate protein adsorption.

Currently, numerous techniques are used to immobilize PEG chains onto surfaces to elucidate the interaction between proteins and PEG chains, including self-assembled monolayers,[25] chemical coupling,[26] and graft polymerization.[27,28] For the fabrication of PEG-grafted polyolefin surfaces, efforts have been exerted to introduce a polyethylene (PE) copolymer containing acrylic acid residues as substrates for esterifying reaction with poly(ethylene glycol) methyl ether (mPEG). Poly(ethylene-co-acrylic acid) (PEAA) is a polymer with a nonpolar polymer scaffold that contains a small amount of polar groups. Previous studies have used PEAA as a solid support for studying the process of enzyme immobilization on polymeric materials[29] and covalent tethering of alkylamino-modified DNA for hybridization analysis.[30]

In this paper, mPEG with two different molecular weights was grafted on polyethylene as a model elucidating the adsorption mechanisms of plasma protein with QCM-D. PE-g-mPEG with different mPEG-grafted densities was fabricated and evaluated by platelet adhesion, whole blood clotting time, and hemolysis rate. The experimental procedure of protein adsorption kinetics included two different schemes, namely, injecting BSA and adding Fib (Scheme 1) and switching the injection order of the two proteins (Scheme 2). A dynamic analysis was performed to elucidate the roles of preadsorption BSA/Fib and protein adsorption mechanism on different PEG surface coverage substrates and wetting property surfaces, respectively.

2. EXPERIMENTAL SECTION

2.1. Materials. Poly(ethylene-co-acrylic acid) (PEAA) (15% w/w acrylic acid) and poly(ethylene glycol) methyl ether (mPEG) (average M_w = 350 750) were purchased from Sigma-Aldrich Co. Di-*n*-octyl phthalate (DOP) and methanol were purchased from Beijing Chemical Factory of China. Bovine serum albumin (05470) and fibrinogen (F8630) were obtained from Sigma Chemical Co. Phosphate-buffered saline (PBS 0.9% NaCl, 0.01 M phosphate buffer, pH 7.4) used for protein adsorption and hemocompatibility experiment was freshly prepared. The amount of static protein adsorption was determined using a Micro BCATM protein assay reagent kit (AR1110, Boster Biological Technology, Co., Ltd., Wuhan, China). Other reagents were AR grade and used without further purification.

2.2. Preparation of PE-g-mPEG. Monomethoxy poly(ethylene glycol) (mPEG) with different molecular weights was grafted onto PEAA through the esterification reaction of carboxyl groups on PEAA with the hydroxyl end group in mPEG. The details of the preparation, chemical composition characterization, contact angle, and surface energy analysis are described in the Supporting Information (SI).

2.3. Blood Compatibility Test. *2.3.1. Static Protein Adsorption Test.* The modified film measuring 1 cm × 1 cm was initially washed with PBS solution for 8 h and then immersed in PBS (0.01 M, pH 7.4) of 1.0 mg/mL BSA for 120 min at 37 °C. The films were rinsed five times with PBS. The adsorbed protein was detached using sodium dodecyl sulfate (SDS) (1 wt % in water) by sonication for 20 min. The amount of adsorbed proteins on the membrane surface was calculated from the concentration of proteins in the SDS solution using a Micro BCA protein assay reagent kit.[31,32] The concentrations were determined based on the absorptiometer at 570 nm using TECAN (TECAN GENIOS, Austria). The reported data were the mean values of triplicate specimens for each film.

Tapping-mode atomic force microscopy was performed to identify surface topography of protein adsorption on a Seiko SPA-300HV microscope with an SPI 3800N controller. Etched silicon cantilevers with a spring constant of 42 N m^{-1} were used.

2.3.2. Platelet Adhesion Test. Fresh blood collected from a healthy rabbit was immediately mixed with a 3.8 wt % solution of sodium citrate at a dilution ratio of 9:1 (blood/sodium citrate solution). The diluted blood was performed in all blood compatibility tests. The blood was centrifuged at 1000 rpm for 10 min at 8 °C to obtain the platelet-rich plasma (PRP). The film (1 cm × 1 cm) was introduced with 100 μL of PRP, and then incubated at 37 °C for 2 h under a static state. After incubation, the film was again rinsed with PBS three times to remove any nonadhering platelets. The film was transferred to new wells. Subsequently, the film was immersed in PBS solution containing 2.5 wt % glutaraldehyde for 8 h at 4 °C to set the adhered platelets. After thorough washing with deionized water three times, the platelets were dehydrated with 30%, 50%, 70%, 90%, and 100% (v/v) ethanol/water solution for 30 min each in sequence, and then naturally dried in the air. A sample was then gold sputtered in vacuum and observed by field-emission scanning electron microscopy (FESEM, XL 30 ESEM FEG, FEI Company).[33]

2.3.3. Whole Blood Clotting Time Test. The anticoagulant property of PEAA and PE-g-mPEG was evaluated using fresh rabbit blood by the kinetic clotting time method. The film (1 cm × 1 cm) was placed in a thermostat at 37 °C for 5 min, and then 80 μL of diluted blood was dropped on the surface of the film. The blood sample was added with 10 μL of $CaCl_2$ solution (0.08 M). After 5, 10, 20, and 30 min incubation at 37 °C in a constant-temperature oven, 5 mL of deionized water was added to stop the clotting. The free hemoglobin was then dispersed in water. The concentration of this free hemoglobin in water was measured by monitoring the absorbance at 540 nm using a spectrophotometer. The relative absorbency of 80 μL of whole blood diluted by 5 mL of distilled water was assumed to be 100. The blood clotting index (BCI) of the biomaterial can be quantified by the following equation:[34]

$$\mathrm{BCI} = \frac{\text{Absorbancy of blood which had been in contact with sample}}{\text{Absorbancy of solution of distilled water and fresh blood}} \times 100$$

2.3.4. Hemolysis Rate Test. The film (1 cm × 1 cm) was immersed in diluted blood solution containing 2% fresh anticoagulated rabbit blood and 98% physiological salt solution, and then incubated at 37 °C for 1 h. After centrifugation at 3000 rpm for 5 min, the absorbance of the solution was recorded as D_t. Under similar conditions, the solution containing 2% fresh anticoagulated rabbit blood and 98% physiological salt solution was used as negative reference, whereas the solution containing 2% fresh anticoagulated rabbit blood and 98% distilled water was used as positive reference. These absorbances were recorded as D_{nc} and D_{pc}, respectively. The hemolysis rate α of the films was calculated using the following formula:[35]

dx.doi.org/10.1021/la4017239 | Langmuir 2013, 29, 6624−6633

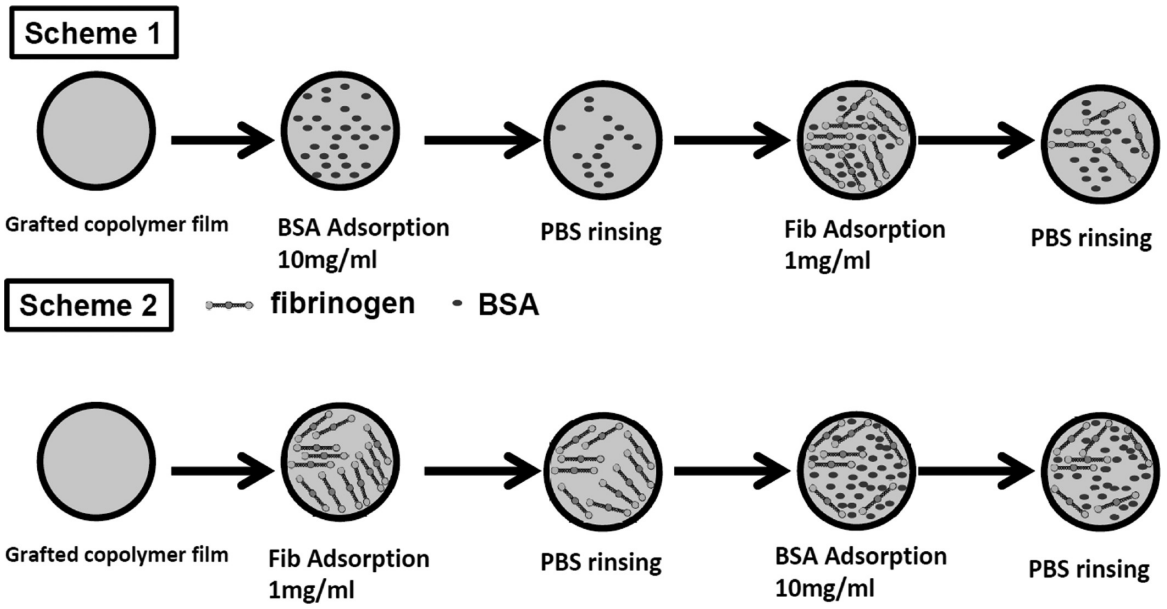

Figure 1. Schematic diagram illustrating protein adsorption kinetics on copolymer film.

$$\alpha = \frac{D_t - D_{nc}}{D_{pc} - D_{nc}} \times 100$$

2.4. Protein Adsorption Kinetics Assays. Protein adsorption kinetics assays were performed on a QCM-D E4 instrument (Q-Sense, Gothenburg, Sweden) with a 4-sensor chamber allowing four parallel measurements. The changes in frequency (Δf) and dissipation (ΔD) were from the third overtone (n = 3) on 5 MHz gold crystals, which presented information on the protein adsorption and structure transition on the grafted layer with adsorbed protein. The mass calculated using the Sauerbrey relation was expected to be an underestimation of the actual mass on PEG-modified surfaces because the films had viscoelastic properties.[36] Thus, the adsorbed mass of proteins was modeled using the Voigt model.

Each PE-g-PEG film or PEAA film was spin-coated on one side of the gold sensor disk from a 5 mg/mL THF solution at 2500 rpm. Prior to its application, the film was heated with the sensor in an oven at 50 °C for 24 h. All experiments were performed at 25 °C (±0.05 °C). Temperature was controlled by the instrument.

Two different schemes were employed to monitor the procedure of protein adsorption kinetics. The details of the steps taken are described in Figure 1. The QCM-D cell was thoroughly rinsed with PBS buffer between each measurement. After stabilization of the baseline in PBS, BSA in PBS was injected with a concentration of 10 mg/mL, and then rinsed off using the PBS solution. Thereafter, another plasma protein was tested by injecting 1 mg/mL Fib in PBS, and then rinsing with buffer. The other scheme was performed by switching the order of injected BSA and Fib. The concentration ratio of the two proteins depended on the proportion in the plasma protein. For each condition, the experiments were repeated multiple times. A representative data set was then presented.

3. RESULTS AND DISCUSSION

3.1. Wettability of PE-g-mPEG Films. Water and ethylene glycol were used to investigate the surface wettability (Figure 2). Table 1 summarizes the calculated results of the surface free energy and components of PEAA film as well as the modified films based on the contact angles of water and ethylene glycol. The water contact angle of PEAA is approximately 94°, which is close to the value of PE. This result indicates that the major component on the PEAA film is hydrophobic PE. Moreover, the acrylic acid surface coverage is low. The lower polar component of the PEAA film surface in Table 1 also confirms

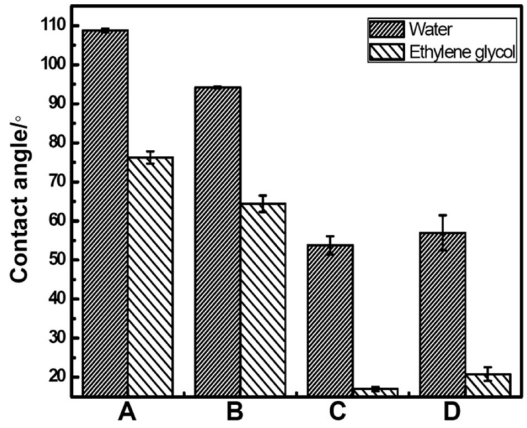

Figure 2. Static water and ethylene glycol contact angles of (A) PE, (B) PEAA, (C) PE-g-mPEG350, and (D) PE-g-mPEG750.

Table 1. Surface Energy Analysis of PE, PEAA, and Modified Copolymers

sample	dispersive component (dyn/cm)	polar component (dyn/cm)	surface energy (dyn/cm)
PE	28.4	0.00072	28.4
PEAA	26.7	1.9	28.6
PE-g-mPEG350	22.9	25.9	48.7
PE-g-mPEG750	24.3	22.6	46.8

the low surface coverage of acrylic acid. Compared with unmodified PEAA, the surface wettability of PE-g-mPEG350 and PE-g-mPEG750 films has been considerably improved, as shown by the contact angles of both water and ethylene glycol. The smallest water contact angle of 54° and ethylene glycol contact angle of 20° are obtained from PE-g-mPEG350, indicating that the surface of PE-g-mPEG350 has the best hydrophilicity. In fact, the polar component of the modified films decreases gradually as the mPEG molecular weight of 350 increases to 750. All these results can be attributed to the surface coverage of mPEG, which was determined by X-ray photoelectron spectroscopy (Table 2). The surface coverage of

dx.doi.org/10.1021/la4017239 | Langmuir 2013, 29, 6624−6633

PE-g-mPEG350 is 1.65%, which is approximately 4-fold that of PE-g-mPEG750.

Table 2. Graft Density and Surface Coverage of Modified Copolymers

	PE-g-mPEG350	PE-g-mPEG750
grafted density (%)[a]	1.17	0.67
surface coverage (%)[b]	1.65	0.43

[a]The grafted degree of mPEG was calculated from ^{1}H NMR (SI). [b]The surface coverage of mPEG was calculated from the XPS analysis (SI).

3.2. Evaluation of Blood Compatibility. *3.2.1. Static Protein Adsorption.* Protein adsorption on modified copolymer surfaces is measured using BSA as model protein. The static BSA adsorbed amount of PEAA reaches 6.0 μg/cm^2, whereas that of the modified PE-g-mPEG350 and PE-g-mPEG750 is 1.1 and 2.8 μg/cm^2, respectively (Figure 3).

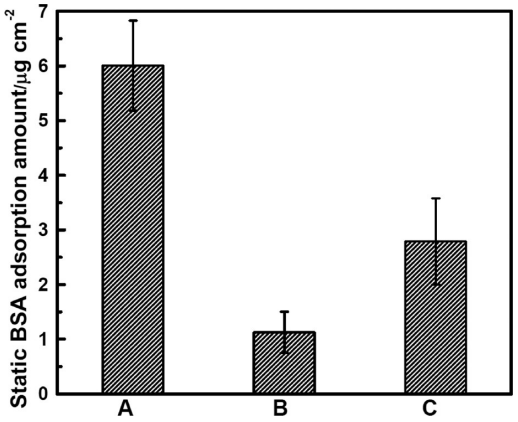

Figure 3. Static BSA adsorption amounts of (A) PEAA, (B) PE-g-mPEG350, and (C) PE-g-mPEG750.

Modified PE-g-mPEG significantly diminishes the overall amount of adsorbed BSA. Our obtained test value on the protein-adsorbed amount is larger than those reported by others.[37,38] This difference may be a result of the test method and the reaction between the surface of PEAA and BSA that can induce a large number of BSA adsorption. The surface coverage of PEG on the modified films decreases with the increase of PEG chain length under similar experimental conditions. Although PEG750 has a larger molecular weight than PEG350, the surface coverage of PE-g-mPEG350 (1.65%) is considerably larger than that of PE-g-mPEG750 (0.43%). PE-g-mPEG350 with shorter chain length is more effective in preventing protein adsorption, because higher PEG surface coverage could depress the hydrophobic interaction between the PE-g-mPEG350 surface and the interacting protein. Thus, BSA protein adsorption decreases with the increase of PEG surface coverage. In addition, the surface morphologies of the films affect protein adsorption. The surface topographies of PEAA and the modified films before and after static BSA protein adsorption are shown in Figure 4. The surfaces of PE-g-mPEG350 and PE-g-mPEG750 have obvious microphase-separated domain structures. The amount of BSA proteins aggregated on the surfaces of the modified films significantly decreases. A possible explanation for the BSA adsorption difference between PEAA and the modified films is the ability of the submicrometer microphase-separated structures to improve their blood compatibility.[39,40] Clearly, different molecular weight grafted copolymers have different surface topographies. These differences ultimately affect the result of protein adsorption. Evident topographical changes in the PE-g-mPEG350 film were observed before and after static BSA protein adsorption. The PEG chains possibly regulate their conformation to maintain the native conformation of BSA in PBS, which leads to surface topographical changes and low protein adsorption level.[41]

3.2.2. Platelet Adhesion. When a surface is exposed to blood, plasma proteins are rapidly adsorbed on the surface, followed by platelet adhesion and activation, coagulation, complement activation, and other blood cell responses.[42,43] Figure 5 shows the SEM images of platelets that adhered on the PEAA and modified film surfaces. The platelets that adhered on the PEAA surface are highly activated with spread, aggregation,

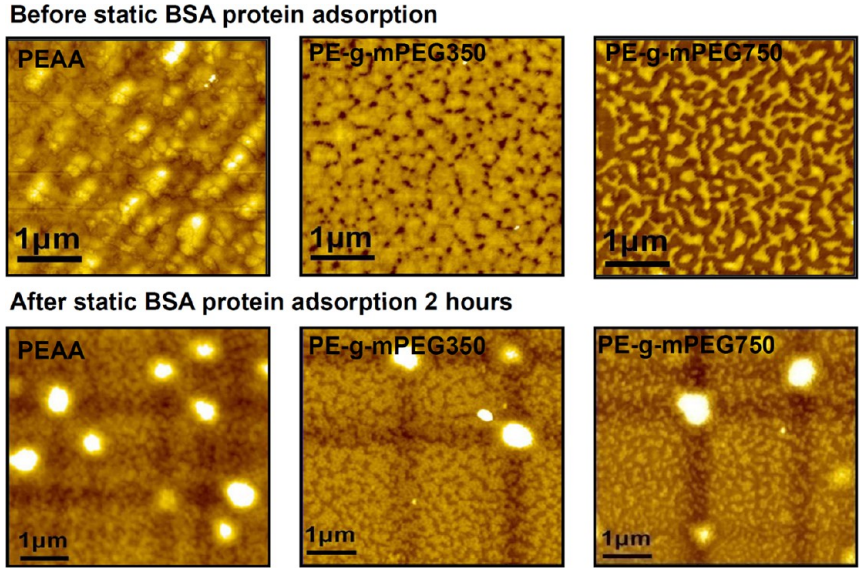

Figure 4. Surface morphologies of PEAA and modified films before and after static BSA protein adsorption.

dx.doi.org/10.1021/la4017239 | *Langmuir* 2013, 29, 6624−6633

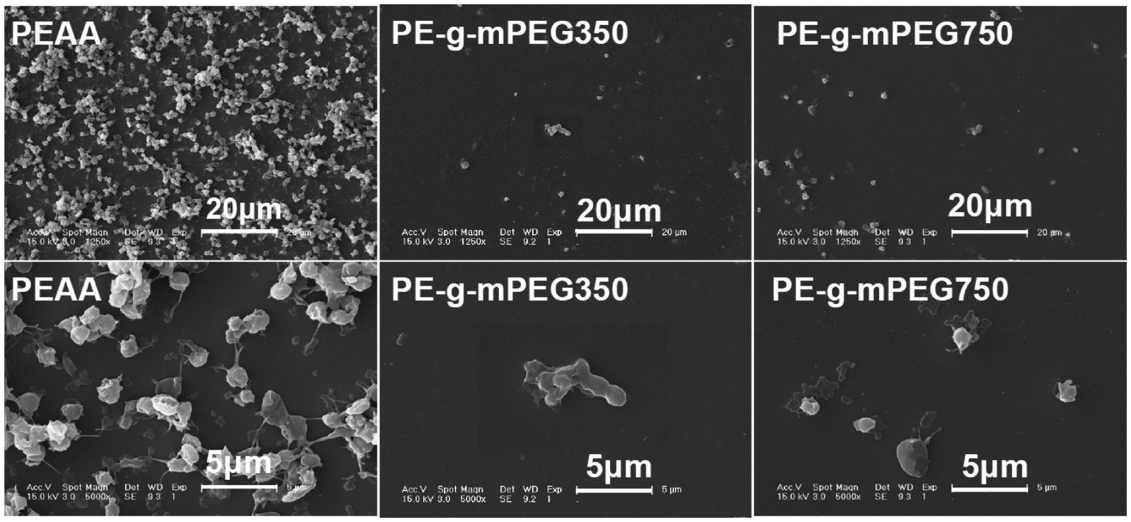

Figure 5. SEM images of platelets that adhered on PEAA and modified films surfaces.

and pseudopodia states. In contrast, the platelets that adhered on the surfaces of modified films maintain their original round shape and the number of platelets dramatically decreases. Figure 5 shows that the number of platelets that adhered to PE-g-mPEG350 is considerably fewer than the number of those that adhered to PE-g-mPEG750, which is consistent with the results of protein adsorption (Figure 3). The results of platelet adhesion prove that the hemocompatibilities of copolymer films are improved effectively. Moreover, the hemocompatibility of PE-g-mPEG350 is better than that of PE-g-mPEG750.

3.2.3. Blood Clotting and Hemolysis. The anticoagulant property is represented by BCI, that is, the absorbency ratio of the blood solution that came in contact with the sample to the absorbency of the fresh blood solution. Under the same condition, a larger BCI surface indicates better anticoagulant property. Figure 6 shows the effect of the blood contact time of

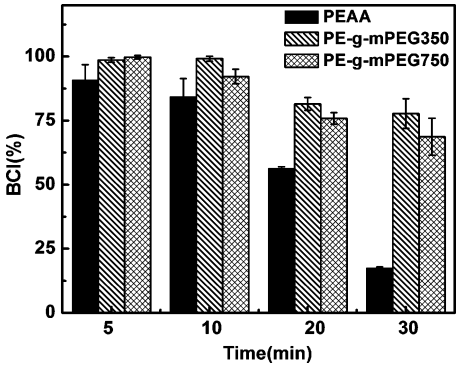

Figure 6. Blood clotting index changes of PEAA, PE-g-mPEG350, and PE-g-mPEG750 films with time (mean ± SD, $N = 5$).

PEAA and modified films on BCI. The BCI of PEAA swiftly declines to 17% in 30 min, whereas the BCI of the modified films remains above 75%. These results indicate the significant improvement on the anticoagulant properties of PE-g-mPEG films. The most influential factors for the anticoagulant property of modified films are the hydrophilic PEG molecules, which can resist plasma protein adsorption, inhibit the intrinsic coagulation cascade, mediate platelet attachment and activation, and ultimately prevent clotting.

Hemolysis rate is an important parameter for evaluating blood compatibility. The ratio represents the extent of the red blood cell rupture caused by the release of hemoglobin. The better hemocompatibility of the biomaterial is characterized by a lower hemolysis rate. The hemolysis rates of the PEAA and modified films are shown in Figure 7. The hemolysis rates of

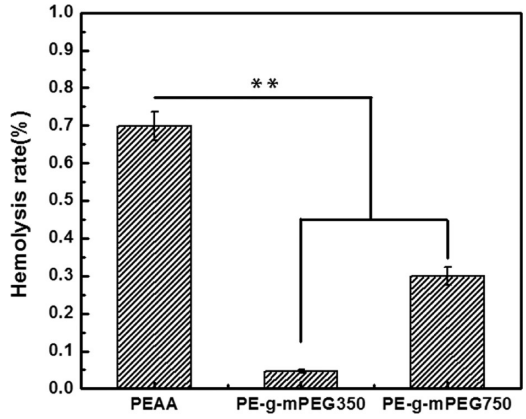

Figure 7. Hemolysis rate of PEAA, PE-g-mPEG350, and PE-g-mPEG750 (**$p < 0.05$ compared with PEAA; mean ± SD, $N = 8$).

PE-g-mPEG350 and PE-g-mPEG750 films are observed to be significantly lower than that of PEAA ($p < 0.05$). The hemolysis rates of the three samples are all below 1%. The obtained $p <$ 0.1% for the PE-g-mPEG350 film implies the best blood compatibility of the PE-g-mPEG350 surface in this study.

3.3. Protein Adsorption Kinetics. The variations in protein adsorbed mass over time with two different schemes are given in Figure 8. PE-g-mPEG350 has the lowest BSA and Fib adsorbed amount in Scheme 1 (BSA injected first, followed by Fib) (Figure 8A). By contrast, all samples have nearly the same amount of adsorbed Fib. Moreover, the modified films have the same final adsorbed amounts in Scheme 2 (Fib injected first, followed by BSA) (Figure 8B). This result indicates that different sequences of injection have completely divergent protein adsorption mechanisms, which can be attributed to the different physicochemical properties and the opposite effect on thrombosis of BSA and Fib. BSA has thromboresistant ability, whereas Fib is an adhesive protein

dx.doi.org/10.1021/la4017239 | *Langmuir* 2013, 29, 6624−6633

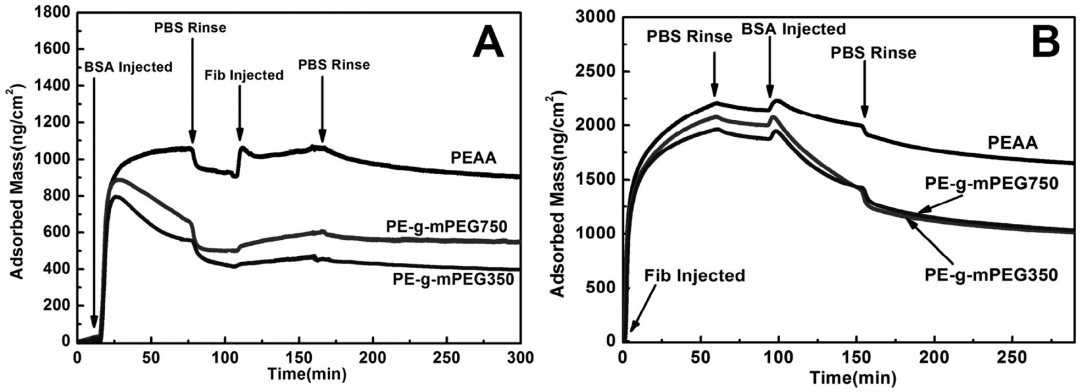

Figure 8. QCM-D traces showing the dynamic protein adsorbed mass of copolymers in (A) Scheme 1 and (B) Scheme 2.

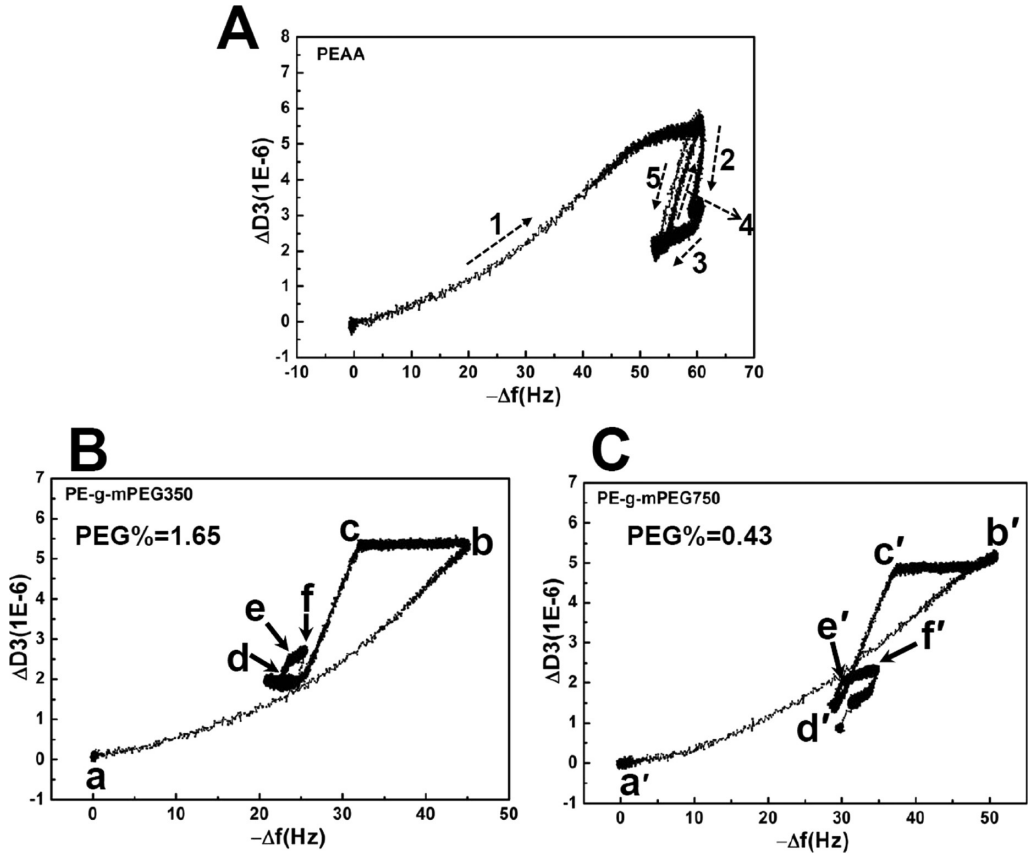

Figure 9. ΔD vs Δf relation in Scheme 1 for (A) PEAA, (B) PE-g-mPEG350, and (C) PE-g-mPEG750.

with a significant role in coagulation and platelet activation and aggregation. The theoretical adsorption amounts of BSA on a surface in the end-on and side-on close-packed monolayer surface coverage are 720 and 210 ng/cm^2, respectively.[44] The amount of BSA adsorbed on the PEAA surface after buffer rinsing is higher than the theoretically calculated value in the end-on orientation (Figure 8A, in Scheme 1). The adsorbed BSA on the surface of PEAA is assumed to form a multilayer. By contrast, BSA adsorbed on the surfaces of PE-g-mPEG350 and PE-g-mPEG750 is a mixture of side-on and end-on orientations because the adsorbed amounts are 400 and 500 ng/cm^2, respectively. When BSA is adsorbed on the modified surfaces from the solution, the adsorbed amount reaches its maximum value transiently, and then continues to decrease gradually, especially with buffer rinsing. The loose coupling of BSA on the modified surface is easier to rinse because the interaction between BSA and modified surfaces is weaker than that between BSA and PEAA. In addition, the results prove that PEG chains have excellent resistance to nonspecific BSA adsorption. Furthermore, the subsequent injection of Fib does not increase the adsorbed protein amounts on the modified film surfaces, indicating that the BSA adsorbed on surfaces of the modified films can effectively inhibit the adsorption of Fib. The conformation of BSA adsorbed on the surface of PEAA changes because of the interface-induced denaturation of proteins.[45] Hydrophobic interaction is dominated when BSA attaches to the surface of PEAA. BSA rearranges its structure to reach an energetically advantageous conformation, and then presents the hydrophobic side chains at the exterior from the interior part of BSA, leading to its partial or total denaturation.

dx.doi.org/10.1021/la4017239 | *Langmuir* 2013, 29, 6624−6633

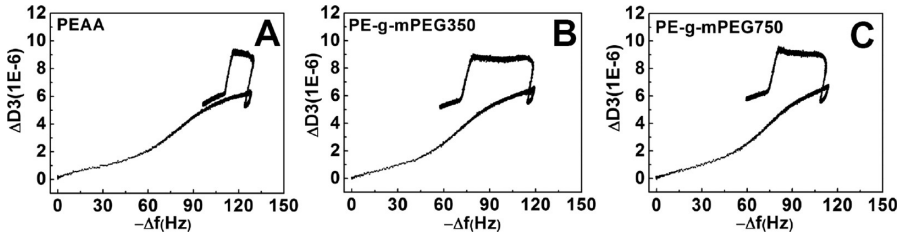

Figure 10. ΔD vs Δf relation in Scheme 2 for (A) PEAA, (B) PE-g-mPEG350, and (C) PE-g-mPEG750.

Thus, the denatured BSA can continuously induce the subsequent adsorption of Fib. However, when BSA is adsorbed on the hydrophilic PEG chains, BSA on the surface of the modified copolymers could preserve the hydrophilic and hydrophobic side chains at the exterior and interior parts, respectively. Thus, BSA protein has the same conformation as in aqueous solution. The diffusional hydrophilic layer may be formed between the adsorbed BSA and the solution interface, which can resist the subsequent adsorption of Fib.

If Fib is injected first, followed by the addition of high-concentration BSA (BSA/Fib = 10/1 mol/mol) (Figure 8B), BSA can gradually displace Fib in the solution with lower concentration. After the injection of BSA, the adsorbed amounts continue to decline gradually. This finding reflects that the displacement is accompanied by flowing solution flushing. The adsorbed amount of Fib on the modified hydrophilic surfaces achieves coverage above 100 ng/cm^2. Thus, Fib cannot fully spread and start to partly overlap,[46] resulting in an increase in the exchange probability of the smaller BSA molecules compared with the hydrophobic PEAA surface.

Figure 9 shows the relationship between ΔD and $-\Delta f$ of PEAA, and the modified films obtained in Scheme 1. In general, an increase in $-\Delta f$ indicates an increase in the coupled mass to the quartz crystal, whereas an increase in ΔD indicates increased viscous loss to the adsorbed layers. The linear relationship between ΔD and $-\Delta f$ indicates that no conformational changes occur during the adsorption process.[36,47] However, a distinct difference exists between the PEAA and modified film surfaces in terms of the patterns of ΔD and $-\Delta f$ (Figure 9). As shown in Figure 9A, ΔD increases as $-\Delta f$ increases on the surface of PEAA. However, no obvious platform exists when it is compared with Figures 9B and 9C. This phenomenon may be attributed to the absence of hydrophilic PEG molecule chains on the surface of PEAA, which repress the changes in ΔD and $-\Delta f$ during BSA adsorption.

Figure 9B and 9C show the relationship of ΔD and $-\Delta f$ obtained in Scheme 1 on the surfaces of PE-g-mPEG350 and PE-g-mPEG750. Moreover, the surface coverage of mPEG is 1.65% and 0.43%, respectively. BSA is first injected into the chamber (Figure 9B a to 9B b]. Then, ΔD increases sharply with the increment of $-\Delta f$, indicating that the BSA molecules are adsorbed on the PEG surface. As shown in Figure 8A, the adsorption is rapid. Additionally, the adsorbed mass changes sharply within 5 min. However, the curve in Figure 9B shows a platform (Figure 9B b to 9B c), indicating that $-\Delta f$ keeps decreasing and ΔD remains unchanged. The balance of the PEG brush partly collapses, and BAS adsorption renders ΔD constant. The contribution of PEG chain dehydration to $-\Delta f$ is larger than that of BAS adsorption, leading to a reduction in the value of $-\Delta f$. To maintain the natural conformation of the approaching BSA and to resist protein adsorption, the PEG chains change their conformation, and then make ΔD constant. The results provide a significant molecular mechanism for elucidating the interaction between PEG chains and plasma proteins when PEG-modified biomaterials are in contact with blood. If a protein molecule attempts to compress this hydrated PEG chain, a loss in the conformation entropy of the PEG chain ensues. This entropy loss can generate a repulsive interaction between the protein molecule and the PEG chain. The value of this loss can be expressed as $T\,(\Delta S/\Delta l)_{T,V}$, where T is temperature, ΔS is the entropy loss, and Δl is the PEG chain deformation induced by the compression. The existence of this repulsive interaction pushes the PEG chain to resist the protein approach. Rinsing with PBS (Figure 9B c−d) washes away the BSA proteins. Thus, ΔD gradually diminishes with decreasing $-\Delta f$. As shown in Figure 9B and 9C, the desorption rate of BSA is larger than that of adsorption. The buffer rinse increases the flexibility of the PEG chains on both PE-g-mPEG350 and PE-g-mPEG750, which is associated with dissipation. However, a distinct platform is found in the rinse of the PE-g-mPEG350 film, whereas the PE-g-mPEG750 film shows a linear relationship between ΔD and $-\Delta f$. This phenomenon can be ascribed to the conformational changes of the polymer chain from pancake-like to mushroom-like conformation and mushroom-to-brush transition, as predicted by the Alexander−de Gennes theory of grafted polymer.[48] The PEG surface coverage of PE-g-mPEG350 is roughly 4-fold compared with that of PE-g-mPEG750. PEG chains can form a polymer brush structure on the PE-g-mPEG350 surface because of the balance between segment−segment repulsion and chain elasticity, whereas the PEG chains with low surface coverage on the surface of PE-g-mPEG750 may exhibit a pancake-like structure.[49] When BSA molecules are adsorbed on the surface of PE-g-mPEG350, not all detached water molecules can leave the PEG brush immediately. Some molecules are trapped in the dense PEG brush. After rinsing with PBS, BSA molecules are desorbed from the surface, accompanied by a decline in ΔD and $-\Delta f$. Then, the trapped water molecules gradually diffuse out of the brush, leading to a decrease in $-\Delta f$. The dense PEG brush on the surface of PE-g-mPEG350 keeps ΔD unchanged. From the perspective of entropy elasticity, the release of trapped water is an important increase of entropy, which should lead to an increase in ΔD. However, the dense PEG brush tightens owing to the release of water. This phenomenon can result in a decrease in the conformational entropy of PEG chains, thus decreasing ΔD. Therefore, the balance between the release of trapped water and the collapse of PEG chain keeps ΔD unchanged. By contrast, the trapped water molecules in the pancake-like structure of PEG chains on the surface of PE-g-mPEG750 are released completely to resist BSA adsorption. In conclusion, the surface coverage, not the chain length of PEG, is vital to the nonspecific protein adsorption of BSA. This

dx.doi.org/10.1021/la4017239 | Langmuir 2013, 29, 6624−6633

conclusion may be attributed to the dense PEG brush on the surface of PE-g-mPEG350, which can release more trapped water molecules to resist BSA adsorption. During the subsequent Fib injection (Figure 9B d–e), ΔD increases sharply as $-\Delta f$ increases. The adsorption process (Figure 9B e–f) exhibits a much smoother gradient, demonstrating that the adsorption rate slows down gradually. The elongated Fib tends to rearrange and pack more densely.[50] Thus, the modified surfaces form either a more shrinkable structure or a denser binding between Fib and PEG molecules.

Figure 10 shows the relationship between ΔD and $-\Delta f$ obtained in Scheme 2 of the PEAA and modified films. The curves of the PEAA and modified films exhibit similar trends, but the lengths of their platforms are different. PE-g-mPEG350 has the longest platform length, PE-g-mPEG750 has a moderate length, and PEAA has the shortest length. This result corresponds to the amounts of Fib displaced by BSA (Figure 8B). Fib displacement rates on the hydrophilic surface of PE-g-mPEG350 (water contact angle = 54°) and PE-g-mPEG750 (water contact angle = 58°) are greater than 95° of the hydrophobic surface of PEAA, which can be inferred from the slopes in Figure 8B. The amounts of Fib displacement depend on the surface wettability of the films (Figure 2). Consequently, the mechanisms for Fib displacement on hydrophobic and hydrophilic surfaces are quite different. On the surface of hydrophobic PEAA, Fib changes its conformation to form denser structures because of strong hydrophobic interactions. The inactivated and denatured Fib is hardly displaced by BSA. Conversely, the electrostatic interactions between Fib and the hydrophilic surfaces could cause the former to partly spread out and overlap. A repulsive salvation force caused by strongly bonded water molecules is mostly presented.[51] Thus, the displacement is available. Therefore, surface hydrophilicity has a significant effect on Fib displacement.

4. CONCLUSIONS

We fabricated different PEG-grafted densities of PE-g-mPEG, and then evaluated their hemocompatibility by static BSA adsorption, platelet adhesion, whole blood clotting time, and hemolysis rate. Hemocompatibility of the copolymer films is improved effectively. PE-g-mPEG350 with high PEG surface coverage has superior hemocompatibility. The protein adsorption mechanisms in two different schemes revealed that the preadsorbed BSA on the surfaces of hydrophilic-modified films could inhibit subsequent Fib adsorption effectively, and that preadsorbed Fib could be gradually displaced by high-concentration BSA.

With the preadsorbed BSA scheme, the surface coverage, not the chain length of PEG, is found to be vital to the nonspecific protein adsorption of BSA. On one hand, the PEG chains change their conformation to resist the perturbations on the native conformations of the interacting BSA caused by the surfaces. On the other hand, the dense PEG brush on the surface of PE-g-mPEG350 could release more trapped water molecules to resist BSA adsorption. With the preadsorbed Fib scheme, the inactivated and denatured Fib is hardly displaced by BSA on the surface of hydrophobic PEAA. However, Fib could be partly spread out and overlapped because of the electrostatic interactions between the Fib and hydrophilic surfaces. Therefore, the adsorption and displacement of Fib depend on the surface hydrophilicity of biomaterials.

Combined acquisition of frequency and dissipation changes with the passage of time was exploited to detect the binding behavior, conformational change, and interactions between approaching proteins and PEG chains. Hydrophobic and electrostatic interactions are the main driving forces when proteins move to a surface. The wettability of a surface determines which force will have a dominant role in destroying the tertiary structure of the protein.

■ ASSOCIATED CONTENT

Supporting Information

Methods used to prepare PE-g-mPEG, and the FTIR, ^{1}H NMR, XPS characterizations and contact angle and surface energy analysis for PE-g-mPEG. This material is available free of charge via the Internet at http://pubs.acs.org.

■ AUTHOR INFORMATION

Corresponding Author

*Fax: +86-431-85262126; tel: +86-431-85262151; e-mail: wjiang@ciac.jl.cn (W.J.); yinjh@ciac.jl.cn (J.Y.).

Notes

The authors declare no competing financial interest.

■ ACKNOWLEDGMENTS

We acknowledge the financial support of the National Natural Science Foundation of China (Projects 51273199, 50920105302, and 21274150). The work was carried out in accordance with the framework of the Research Cooperation Agreement between the Chinese Academy of Sciences and the National Research Council of Italy.

■ REFERENCES

(1) Xu, K.; Ouberai, M. M.; Welland, M. E. A comprehensive study of lysozyme adsorption using dual polarization interferometry and quartz crystal microbalance with dissipation. *Biomaterials* **2013**, *34* (5), 1461–1470.

(2) Deutsch, S.; Tarbell, J. M.; Manning, K. B.; Rosenberg, G.; Fontaine, A. A. Experimental fluid mechanics of pulsatile artificial blood pumps. *Annu. Rev. Fluid Mech.* **2006**, *38*, 65–86.

(3) Pitt, W. G.; Park, K.; Cooper, S. L. Sequential protein adsorption and thrombus deposition on polymeric biomaterials. *J. Colloid Interface Sci.* **1986**, *111* (2), 343–362.

(4) Rodrigues, S. N.; Gonçalves, I. C.; Martins, M.; Barbosa, M. A.; Ratner, B. D. Fibrinogen adsorption, platelet adhesion and activation on mixed hydroxyl-/methyl-terminated self-assembled monolayers. *Biomaterials* **2006**, *27* (31), 5357–5367.

(5) Wu, J.; Mao, Z.; Gao, C. Controlling the migration behaviors of vascular smooth muscle cells by methoxy poly(ethylene glycol) brushes of different molecular weight and density. *Biomaterials* **2012**, *33* (3), 810–820.

(6) Leckband, D.; Sheth, S.; Halperin, A. Grafted poly (ethylene oxide) brushes as nonfouling surface coatings. *J. Biomater. Sci., Polym. Ed.* **1999**, *10* (10), 1125–1147.

(7) Halperin, A.; Kroeger, M. Ternary protein adsorption onto brushes: Strong versus weak. *Langmuir* **2009**, *25* (19), 11621–11634.

(8) Alibeik, S.; Zhu, S. P.; Brash, J. L. Surface modification with PEG and hirudin for protein resistance and thrombin neutralization in blood contact. *Colloids Surf. B, Biointerfaces* **2010**, *81* (2), 389–396.

(9) Jin, J.; Jiang, W.; shi, Q.; Zhao, J.; Yin, J.; Stagnaro, P. Fabrication of PP-g-PEGMA-g-heparin and its hemocompatibility: From protein adsorption to anticoagulant tendency. *Appl. Surf. Sci.* **2012**, *258* (15), 5841–5849.

(10) Chen, H.; Yuan, L.; Song, W.; Wu, Z.; Li, D. Biocompatible polymer materials: Role of protein–surface interactions. *Prog. Polym. Sci.* **2008**, *33* (11), 1059–1087.

(11) Larsson, A.; Ekblad, T.; Andersson, O.; Liedberg, B. Photografted poly(ethylene glycol) matrix for affinity interaction studies. *Biomacromolecules* **2007**, *8* (1), 287−295.
(12) Jeon, S.; Andrade, J. Protein−surface interactions in the presence of polyethylene oxide: II. Effect of protein size. *J. Colloid Interface Sci.* **1991**, *142* (1), 159−166.
(13) Jeon, S.; Lee, J.; Andrade, J.; De Gennes, P. Protein−surface interactions in the presence of polyethylene oxide: I. Simplified theory. *J. Colloid Interface Sci.* **1991**, *142* (1), 149−158.
(14) Hasegawa, M.; Kitano, H. Adsorption kinetics of proteins onto polymer surfaces as studied by the multiple internal reflection fluorescence method. *Langmuir* **1992**, *8* (6), 1582−1586.
(15) Kasemo, B.; Gold, J. Implant surfaces and interface processes. *Adv. Dental Res.* **1999**, *13* (1), 8−20.
(16) Kulmashiro, Y.; Ikezoe, Y.; Tamada, K.; Hara, M. Dynamic interfacial properties of poly(ethylene glycol)-modified ferritin at the solid/liquid interface. *J. Phys. Chem. B* **2008**, *112* (28), 8291−8297.
(17) MacRitchie, F. Consequences of protein adsorption at fluid interfaces. In *Proteins at Interfaces*; American Chemical Society: Washington, DC, 1987; Vol. *343*, pp 165−179.
(18) Sadana, A. Protein adsorption and inactivation on surfaces. Influence of heterogeneities. *Chem. Rev.* **1992**, *92* (8), 1799−1818.
(19) Sauerbrey, G. Use of quartz vibration for weighing thin films on a microbalance. *J. Physik* **1959**, *155*, 206−212.
(20) Zwang, T. J.; Patel, R.; Johal, M. S.; Selassie, C. R. Desolvation of BSA−ligand complexes measured using the quartz crystal microbalance and dual polarization interferometer. *Langmuir* **2012**, *28*, 9616−9620.
(21) Höök, F.; Kasemo, B.; Nylander, T.; Fant, C.; Sott, K.; Elwing, H. Variations in coupled water, viscoelastic properties, and film thickness of a Mefp-1 protein film during adsorption and cross-linking: A quartz crystal microbalance with dissipation monitoring, ellipsometry, and surface plasmon resonance study. *Anal. Chem.* **2001**, *73* (24), 5796−5804.
(22) Roach, P.; Farrar, D.; Perry, C. C. Interpretation of protein adsorption: Surface-induced conformational changes. *J. Am. Chem. Soc.* **2005**, *127* (22), 8168−8173.
(23) Guzmán, E.; Cavallo, J. A.; Chuliá-Jordán, R.; Gómez, C. s.; Strumia, M. C.; Ortega, F.; Rubio, R. n. G. pH-Induced changes in the fabrication of multilayers of poly(acrylic acid) and chitosan: Fabrication, properties, and tests as a drug storage and delivery system. *Langmuir* **2011**, *27* (11), 6836−6845.
(24) Guzmán, E.; Ritacco, H.; Rubio, J. E.; Rubio, R. G.; Ortega, F. Salt-induced changes in the growth of polyelectrolyte layers of poly(diallyl-dimethylammonium chloride) and poly(4-styrene sulfonate of sodium). *Soft Matter* **2009**, *5* (10), 2130−2142.
(25) Yang, Z.; Galloway, J. A.; Yu, H. Protein interactions with poly(ethylene glycol) self-assembled monolayers on glass substrates: Diffusion and adsorption. *Langmuir* **1999**, *15* (24), 8405−8411.
(26) Zhang, C.; Luo, N.; Hirt, D. E. Surface grafting polyethylene glycol (PEG) onto poly(ethylene-co-acrylic acid) films. *Langmuir* **2006**, *22* (16), 6851−6857.
(27) Hucknall, A.; Rangarajan, S.; Chilkoti, A. In pursuit of zero: Polymer brushes that resist the adsorption of proteins. *Adv. Mater.* **2009**, *21* (23), 2441−2446.
(28) Ma, H.; Li, D.; Sheng, X.; Zhao, B.; Chilkoti, A. Protein-resistant polymer coatings on silicon oxide by surface-initiated atom transfer radical polymerization. *Langmuir* **2006**, *22* (8), 3751−3756.
(29) Su, X.; Zong, Y.; Richter, R.; Knoll, W. Enzyme immobilization on poly(ethylene-co-acrylic acid) films studied by quartz crystal microbalance with dissipation monitoring. *J. Colloid Interface Sci.* **2005**, *287* (1), 35.
(30) Chong, K. T.; Su, X.; Lee, E. J. D.; O'Shea, S. J. Polyethylene-co-acrylic acid as coating for biosensor application: A quartz crystal microbalance study. *Langmuir* **2002**, *18* (25), 9932−9936.
(31) Zhao, J.; Shi, Q.; Luan, S.; Song, L.; Yang, H.; Shi, H.; Jin, J.; Li, X.; Yin, J.; Stagnaro, P. Improved biocompatibility and antifouling property of polypropylene non-woven fabric membrane by surface grafting zwitterionic polymer. *J. Membr. Sci.* **2010**, *369* (1−2), 5−12.
(32) Seo, J. H.; Matsuno, R.; Konno, T.; Takai, M.; Ishihara, K. Surface tethering of phosphorylcholine groups onto poly(dimethylsiloxane) through swelling−deswelling methods with phospholipids moiety containing ABA-type block copolymers. *Biomaterials* **2008**, *29* (10), 1367−1376.
(33) Xu, F.; Li, Y.; Kang, E.; Neoh, K. Heparin-coupled poly (poly(ethylene glycol) monomethacrylate)-Si (111) hybrids and their blood compatible surfaces. *Biomacromolecules* **2005**, *6* (3), 1759−1768.
(34) Zhou, C.; Yi, Z. Blood-compatibility of polyurethane/liquid crystal composite membranes. *Biomaterials* **1999**, *20* (22), 2093−2099.
(35) Li, G.; Yang, P.; Liao, Y.; Huang, N. Tailoring of the titanium surface by immobilization of heparin/fibronectin complexes for improving blood compatibility and endothelialization: An in vitro study. *Biomacromolecules* **2011**, *12* (4), 1155−1168.
(36) Slavin, S.; Soeriyadi, A. H.; Voorhaar, L.; Whittaker, M. R.; Becer, C. R.; Boyer, C.; Davis, T. P.; Haddleton, D. M. Adsorption behaviour of sulfur containing polymers to gold surfaces using QCM-D. *Soft Matter* **2012**, *8* (1), 118−128.
(37) Higuchi, A.; Sugiyama, K.; Yoon, B. O.; Sakurai, M.; Hara, M.; Sumita, M.; Sugawara, S.-i.; Shirai, T. Serum protein adsorption and platelet adhesion on pluronic-adsorbed polysulfone membranes. *Biomaterials* **2003**, *24* (19), 3235−3245.
(38) Zhao, C.; Liu, X.; Nomizu, M.; Nishi, N. Blood compatible aspects of DNA-modified polysulfone membrane—protein adsorption and platelet adhesion. *Biomaterials* **2003**, *24* (21), 3747−3755.
(39) Imai, Y. Antithrombogenic materials-role of heterogeneous surface microstructure. *Kobunshi* **1972**, *21*, 569−573.
(40) Miwa, Y.; Tanaka, M.; Mochizuki, A. Water structure and polymer dynamics in hydrated blood compatible polymers. *Kobunshi Ronbunshu* **2011**, *68* (4), 133−146.
(41) Andrade, J. D.; Hlady, V.; Feng, L.; Tingey, K. Proteins at interfaces: Principles, problems, and potential. In *Interfacial Phenomena and Bioproducts*; Brash, J. L., Wojciechowski, P., Eds.; Marcel Dekker: New York, 1996; pp 19−55.
(42) Koh, L. B.; Rodriguez, I.; Venkatraman, S. S. The effect of topography of polymer surfaces on platelet adhesion. *Biomaterials* **2010**, *31* (7), 1533−1545.
(43) Sask, K.; McClung, W.; Berry, L.; Chan, A.; Brash, J. Immobilization of an antithrombin−heparin complex on gold: Anticoagulant properties and platelet interactions. *Acta Biomater.* **2011**, *7*, 2029−2034.
(44) Wertz, C. F.; Santore, M. M. Adsorption and relaxation kinetics of albumin and fibrinogen on hydrophobic surfaces: Single-species and competitive behavior. *Langmuir* **1999**, *15* (26), 8884−8894.
(45) Müller, C.; Lüders, A.; Hoth-Hannig, W.; Hannig, M.; Ziegler, C. Initial bioadhesion on dental materials as a function of contact time, pH, surface wettability, and isoelectric point. *Langmuir* **2009**, *26* (6), 4136−4141.
(46) Renner, L.; Pompe, T.; Salchert, K.; Werner, C. Fibronectin displacement at polymer surfaces. *Langmuir* **2005**, *21* (10), 4571−4577.
(47) Höök, F.; Rodahl, M.; Brzezinski, P.; Kasemo, B. Energy dissipation kinetics for protein and antibody-antigen adsorption under shear oscillation on a quartz crystal microbalance. *Langmuir* **1998**, *14* (4), 729−734.
(48) Baekmark, T. R.; Elender, G.; Lasic, D. D.; Sackmann, E. Conformational transitions of mixed monolayers of phospholipids and polyethylene oxide lipopolymers and interaction forces with solid surfaces. *Langmuir* **1995**, *11* (10), 3975−3987.
(49) Zhang, G. Z.; Wu, C. Quartz crystal microbalance studies on conformational change of polymer chains at interface. *Macromol. Rapid Commun.* **2009**, *30* (4−5), 328−335.
(50) Guthold, M.; Liu, W.; Sparks, E.; Jawerth, L.; Peng, L.; Falvo, M.; Superfine, R.; Hantgan, R.; Lord, S. A comparison of the mechanical and structural properties of fibrin fibers with other protein fibers. *Cell Biochem. Biophys.* **2007**, *49* (3), 165−181.
(51) Ostuni, E.; Chapman, R. G.; Holmlin, R. E.; Takayama, S.; Whitesides, G. M. A survey of structure−property relationships of

surfaces that resist the adsorption of protein. *Langmuir* **2001**, *17* (18), 5605−5620.

dx.doi.org/10.1021/la4017239 | *Langmuir* 2013, 29, 6624−6633